



AIAA-2003-4003

An Experimental Study of the Cavity Flow for Closed-Loop Flow Control

Marco Debiasi and Mo Samimy

The Ohio State University
Department of Mechanical Engineering

33rd AIAA Fluid Dynamics Conference and Exhibit
June 23-26, 2003/ Orlando, FL

An Experimental Study of the Cavity Flow for Closed-Loop Flow Control

M. Debiasi and M. Samimy¹

Gas Dynamics and Turbulence Laboratory
 Collaborative Center of Control Science
 The Ohio State University
 Columbus, Ohio 43210
 Samimy.1@osu.edu
 614-292-6988 (Tel)
 614-292-3163 (Fax)

Abstract

We present the results of an experimental investigation conducted as part of a multidisciplinary effort intended to address systematically the problem of closed-loop flow control by assembling expertise from numerical and experimental flow analysis, flow modeling, and control design disciplines. Experiments were conducted using a shallow-cavity flow in a small-scale wind tunnel that can operate continuously in the subsonic regime. We restricted our attention to cavity flow in the Mach number range 0.25-0.5. The flow exhibits the characteristic staging behavior predicted by the semi-empirical Rossiter formula with multiple modes in the Mach number range 0.32-0.38 and a single strong mode in the other flow conditions. A preliminary survey of the velocity at the exit of the compression-driver actuator used for control reveals that this actuator has a non-linear behavior and was little influenced by the local effect of Mach 0.3 main flow. Forcing the Mach 0.3 flow with the actuator indicates that this has good authority over a large range of frequencies, with elimination of the resonant peak observed at some frequencies. We took advantage of this phenomenon to develop a preliminary, logic-based controller that searches the frequency space and maintains the optimal forcing frequency for peak reduction at each Mach number. Optimal frequencies and the corresponding reduced resonance have been obtained for all the flow conditions explored.

1. Introduction

Application of closed-loop control in flow dynamics is by its nature a challenging and fascinating problem. While many significant results have been obtained with open-loop flow control, this technique sometimes lacks the responsiveness or the flexibility needed for application in dynamic flight environments. In contrast, closed-loop flow control, although in its infancy, appears to be the ideal technique for the successful management of flow in many applications due to its adaptability to variable conditions and to its potential for significantly reducing the power required for controlling the flow. For example, Cattafesta et al. (1997) found that closed-loop control of cavity tones requires an order of magnitude less power than open-loop control.

The closed-loop flow control team of the Collaborative Center of Control Science (CCCS) at the Ohio State University (OSU) is a group of researchers from OSU, Air Force Research Laboratory's Air Vehicles Directorate, and the NASA Glenn Research Center. The goal of the team is to develop tools and methodologies that apply closed-loop aerodynamic flow control for manipulating the flow over maneuvering air vehicles and ultimately for controlling the maneuvers of the vehicles themselves. The first step in the team's effort was to select a particular flow field relevant to Air Force applications and to utilize it in the development of various components of closed-loop flow control techniques. The case study chosen is the control of shallow cavity-flow pressure fluctuations which are characterized by

¹ Corresponding author; Samimy1@osu.edu

a strong resonance produced by a natural feedback mechanism similar to that occurring in other flows with self-sustained oscillations (e.g. edge noise, impinging-jet tones, screech noise). In all these cases, shear-layer structures impacting a geometrical discontinuity or obstacle (e.g. the cavity trailing edge) scatter acoustic waves that propagate upstream and reach the shear-layer receptivity region where they tune and enhance the growth and development of shear-layer structures. Very quickly a flow-acoustic loop is established that drives the system to a resonating condition where turbulence structures become robust and generate large pressure fluctuations. In the case of flow over a weapon-bay cavity, these fluctuations can lead to structural damage to the air vehicle or to the stores carried.

Rossiter first developed an empirical formula for predicting the cavity-flow resonant frequencies, today referred to as Rossiter frequencies or modes (1964). He also investigated the concept of a dominant mode of oscillation. Later Rockwell et al. (1978) observed that this dominant mode tends to coincide with that of the natural longitudinal cavity resonance. Williams et al. (2000b) confirmed that Mach numbers at which single mode resonance occurs are located at the intersections of the first longitudinal cavity mode with the second, third or fourth Rossiter modes while Mach numbers for multi-mode resonance fall between the single-mode resonance conditions. Rapid switching between modes has been observed in multi-mode conditions (Cattafesta et al. 1998, Williams et al. 2000b). Joint time-frequency analysis (short time Fourier transform, Morlet wavelet analysis, and bispectral analysis) captures this phenomenon (Cattafesta et al. 1998). The random switching between multiple modes on a rapid time scale places large bandwidth requirements on the actuation scheme and feedback control algorithm (Cattafesta et al. 1998, Williams et al. 2000b). Rockwell et al. (1964) observed that details of the geometry of the cavity leading and trailing edge influence respectively the shear-layer receptivity region and the acoustic-scattering-process region and as such have significant impact on cavity resonance.

Extensive work has been done on controlling the flow over a cavity using passive techniques (geometrical modifications), active control (open-loop forcing of the flow), and finally closed-loop control (sensors and a controller are used to determine the appropriate forcing). The results of these endeavors are encouraging but also indicate that several issues

remain to be solved. For example, suppression of resonant tones is often accompanied by either peak splitting, i.e. creation of a pair of lower-magnitude tones on either side of the suppressed one (Rowley et al. 2002), or peaking, where additional lower magnitude tones appear away from the original tone(s) (Cabell et al. 2002). Therefore many opportunities remain for further advancement of the technology (Gad-el-Hak 2000).

Actuation is a crucial element of any active control work. Actuators for cavity-flow control are divided into two categories, low frequency and high frequency devices. The requirement for low frequency devices is a bandwidth large enough to include the highest Rossiter frequency (Schaeffler et al. 2002). Candidate low frequency actuators include piezoelectric flaps with deflections on the order of the viscous sublayer of the boundary layer approaching the cavity (Kegerise et al. 2002), steady and pulsating blowing jets (Cain et al. 2000), and synthetic jets that add momentum to the flow without mass addition (Williams et al. 2000a&b). Stanek et al. (2002a&b) successfully demonstrated tone suppression across a broad range of frequencies without exciting additional tones at supersonic speeds by using a powered resonance tube, a high frequency fluidic device whose frequency is an order of magnitude greater than the Rossiter modes (Raman et al. 2001a&b, and Kastner and Samimy 2002). These fluidic actuators are not well suited to closed-loop flow control at the present time, as they cannot be phase locked.

In this work we present the experimental results obtained up to date at the Gas Dynamics and Turbulence Laboratory (GDTL) by the CCCS flow-control team. For this purpose a small subsonic wind tunnel with a shallow cavity has been built and tested and the flow resonance in the Mach number range 0.25-0.5 has been explored. The tunnel with the current arrangement can operate continuously up to Mach 1. With the replacement of its converging nozzle with a converging-diverging nozzle, the facility can operate continuously in supersonic regime. A synthetic-jet type of actuation tickling the shear layer at its receptivity region has been adopted for flow control. A titanium-diaphragm compression driver, a music-quality device capable of large bandwidth and great flexibility in the generation of sound, drives the actuator. A preliminary study of the actuator characteristics without and with main Mach 0.3 flow is presented and the effect of the actuation frequency on the Mach 0.3 flow is investigated. From the results

obtained, an initial, logic-based type of controller has been developed that searches in a closed-loop fashion the frequencies that reduce the cavity-flow resonant peaks and then maintains the system in such conditions. The technique performed well in the experimental trials and allowed identification of optimal frequencies for the reduction of resonant peaks in the Mach number range explored.

In the next sections we will introduce the flow facility used in this study and then focus on the measurements of the baseline flows, the behavior of the actuator, the effect of forcing frequency, and the design and use of the logic-based controller for reducing the resonance. In each section we will describe the experimental procedure and present and discuss the most relevant results obtained.

2. Flow facility

A modular, optically accessible experimental facility has been designed and fabricated at the Gas Dynamics and Turbulence Laboratory at The Ohio State University. The facility is of the blow-down type and operates with air supplied by two four-stage compressors. The air is filtered, dried, and stored at 16.5 MPa in two high-capacity tanks. The air is conditioned in a stagnation chamber before entering the test section through a smoothly contoured converging nozzle. The total pressure in the stagnation chamber can be controlled within 0.07% of the test section static pressure of near the ambient pressure. The test section is square with width $W = 50.8$ mm (2 in). The upper wall of the test section is adjustable to compensate for the growth of the boundary layer and of the shear layer. A variable-depth cavity that spans the entire width of the test section is recessed in the floor. In the current experiments, the cavity depth D is 12.7 mm (1/2 in) and its length L is 50.8 mm (2 in) for an aspect ratio $L/D = 4$. A schematic of the test section with the cavity and the actuator is shown in Fig. 1. Large optical windows and numerous ports allow the use of advanced imaging diagnostics as well as of an array of transducers for pressure and velocity measurements. The facility allows continuous operation in the subsonic range with the current converging nozzle, but can easily be adapted to supersonic operation by changing this nozzle with a converging-diverging one.

The actuator is a 2D synthetic-jet type issuing from a high-aspect-ratio converging nozzle embedded in the

cavity leading edge as shown in Fig. 1. The jet exhausts at an angle of 30° with respect to the main flow through a slot of width $W = 50.8$ mm (the cavity span) and height $h = 1$ mm. Actuation is provided by the movement of the titanium diaphragm of a Selenium D3300Ti compression driver whose voltage signal is amplified by a Crown D-150A amplifier. This device is conceptually similar to the unsteady bleed actuator used by Williams et al. (Williams 2000a&b) for a similar purpose and by McCormick (2000) for boundary layer separation control. The compression driver diaphragm is capable of oscillating in the frequency range 1-20 kHz. When used, as it was designed for, connecting it to an acoustic diffuser for sound production, the device has in this range a flat frequency response. When used in connection to a straight tube, the frequencies in the 500-3000 Hz range are exalted. In the rather unconventional arrangement of our experiments, where the compression driver is connected to a highly-converging nozzle, we expect a non-linear behavior where some frequencies are reinforced while other are reduced. This has been verified by the preliminary measurements of the velocity at the exit slot.

3. Cavity-flow measurements

Preliminary static and dynamic measurements of the flow characteristics in the Mach range 0.25-0.4 have been carried out. Measurements of the static pressure at various locations were used to adjust the upper wall so to maintain a uniform pressure close to the ambient value along the test section. Flow velocity profiles have been measured using a miniature pitot probe (0.8 mm tip diameter) traversing the test section in the horizontal and vertical planes 6.35 mm (1/4 in) upstream of the cavity leading edge. The boundary layer thickness at this location is about 2.5 mm both in the vertical and in the horizontal planes and follows a $1/n$ power law profile with $n = 6$. The flow outside of the boundary layer is very uniform across the test section. The Reynolds number based on the cavity step height is 10^5 and based on the boundary layer thickness is 2×10^4 . Further details on the quality of the flow can be found in Samimy et al. (2003). Analogous measurements are planned to verify the quality of the flow above Mach 0.4.

A complete survey of the cavity-flow resonance in the Mach range 0.25-0.5 was performed using a Kulite XTL-190-25A dynamic pressure transducer with

frequency response up to 50 kHz flush-mounted in the middle of the cavity floor, Fig. 1. The corresponding voltage signal was sampled at 200 kHz through a National Instruments PCI-6036E board installed on a Dell Dimension 8200 computer. The signal was bandpass-filtered between 200 and 20,000 Hz to remove spurious frequency components and converted to non-dimensional pressure value relative to the reference pressure 20 μ Pa. Then Sound Pressure Level spectra were derived.

The spectral peaks were compared with the cavity-flow resonant frequencies predicted using the semi-empirical formula developed by Rossiter (1964)

$$St_n = \frac{f_n L}{U_\infty} = \frac{n - \varepsilon}{M_\infty \left(1 + \frac{\gamma - 1}{2} M_\infty^2 \right)^{-1/2} + \frac{1}{\beta}} \quad (1)$$

where n is an integer mode number corresponding to the number of vortices spanning the cavity length L , U_∞ and M_∞ are the freestream velocity and Mach number, ε is the phase lag (in fractions of a wavelength) between the interaction of a large scale structure in the shear layer with the cavity trailing edge and the formation of a corresponding upstream traveling disturbance (phase shift of the acoustic scattering process), and $\beta = U_c / U_\infty$ is the ratio of the convective speed of the disturbance to the freestream velocity. The predicted Rossiter frequencies of our setup ($L = 50.8$ mm) with $\varepsilon = 0.25$ and $\beta = 0.66$ are presented in Fig. 2 as a function of the flow Mach number. Circles in the figure represent the frequency of the resonant peaks measured in our experimental setup. More specifically, closed circles represent dominant peaks, while open circles represent other peaks appearing in multi-mode resonance.

Our experimental setup exhibits strong, single-mode resonance in the Mach number ranges 0.25-0.31 and 0.39-0.5, and multi-mode resonance in the Mach range 0.32-0.38. The pressure spectra at selected Mach numbers shown in Fig. 3 illustrate this point more clearly. At Mach 0.26 and 0.29, Figs. 3 (a) and (b), a single peak dominates the spectrum by as much as 20 dB over the other spectral components. A similar effect is observed at Mach 0.43 and 0.46, Figs. 3 (e) and (f), where a single resonant peak dominates the other components by as much as 30 dB, as expected for these more energetic, higher Mach number flows. Conversely at Mach 0.32 and 0.37,

Figs. 3 (c) and (d), we observe the presence of multiple smaller peaks that do not exceed significantly the other spectral components. Consistent with the observations of Cattafesta et al. (1998) it seems that in multi-mode resonance the energy available for generation of the acoustic tones had been split among the rapidly alternating peaks instead of concentrating on a single large peak.

Figure 4 complements the previous figures by showing the intensity of the dominant peak as function of the flow Mach number. The dotted line in the figure represents the low-frequency noise plateau, i.e. the noise components below 1000 Hz, whose intensity increases almost linearly with Mach number and represents the strongest noise component after the resonant peaks.

4. Velocity measurements at the actuator exit slot

In order to assess the behavior of the actuator without and with an external flow, preliminary velocity measurements at the exit slot were performed using a TSI 1276-10A subminiature hot-film probe connected to a TSI 1750 constant-temperature anemometer. The voltage timetrace from the anemometer was sampled at 200 kHz without filtering and then translated into velocity values according to the calibration curve provided by the manufacturer for the probe-anemometer setup. Measurements were made without and with a main Mach 0.3 flow by placing the probe in the middle of the exit slot, i.e. at equal distance between the upper and the lower nozzle lip. To verify the spanwise uniformity of the jet, measurements were done at the test-section centerline (i.e. 1 in away from both the side-walls) as well as closer to the side-wall but outside the boundary layer (0.25 in from the wall). No difference has been detected between the center and side measurements both without and with the main flow. Figures 5 to 8 summarize the most relevant finding from the hot-film velocity measurements.

Figure 5 and 6 compare excerpts of the velocity timetraces at the exit slot for excitation at 1.6 kHz with 5 V_{rms} excitation voltage, respectively, without and with the Mach 0.3 main flow. Similar timetraces were observed at the other actuation frequencies with velocity values varying with frequency and decreasing at lower excitation voltages. From Fig. 5 we observe first that, although the hot film records absolute velocity values, contrary to what one would expect

there is no indication of zero-velocity crossing. That is, apparently no negative velocity component is recorded in the middle of the exit slot. In fact the overall behavior resembles that recorded by Smith and Glazer (1998) immediately downstream of the exit slot of a piezoelectric-driven synthetic jet where the jet has already lost the sinusoidal momentum fluctuations occurring at the nozzle and exhibits a positive net momentum with peak instantaneous velocities 2-3 times the average one. This behavior can be explained by hypothesizing that in our setup air is entrained in the very proximity of the nozzle lips. This should be clarified by more accurate, specific measurements of the jet velocity at various locations downstream of the exit slot.

More relevant to the present study is to note that the addition of the Mach 0.3 main flow does not alter significantly the velocity timetraces at the exit slot. Comparing Fig. 6 and Fig. 5 it is clear that the effect of the main flow is to superimpose some velocity oscillations and to slightly raise the mean velocity value. This is consistent with our local measurements of the Mach 0.3 flow alone which exhibits local fluctuations of some few m/s (on the average) about a mean value of 6 m/s. Similar behavior has been observed with actuation at lower voltages. However, the effect of the main flow becomes more dominant at lower voltage settings.

Figure 7 shows the variation of the peak and mean velocity at the exit slot as function of the actuation frequency for excitation at $5 V_{rms}$ in absence of the main flow. As expected the actuator behavior is significantly non-linear with several peaks and valleys in the explored range 1-10 kHz. This confirms the preliminary observations of non-linear behavior reported by Samimy et al. (2003) based on measurements of the forcing-flow mean velocity obtained with the miniature pitot probe. The peak velocity values in excess of 20 m/s and the mean velocity values above 5 m/s shown in Fig. 7 at some frequencies compare well with those observed by Chen et al. (2000) and by Guy et al. (2002) using high aspect ratio rectangular synthetic jets. The frequency behavior at lower excitation voltage is similar to that in Fig. 7 but is characterized by smaller velocity values as can be verified in Fig. 8 for the mean velocity measurements. Addition of the Mach 0.3 main flow changes little this behavior for excitation at 4-5 V_{rms} but impacts the behavior at lower voltage settings where the instantaneous values of the velocity

are heavily distorted by the superposition of the structures from the main flow.

5. Effect of actuation frequency on Mach 0.3 resonant flow

Having verified that, at least for operation at higher voltages, the behavior of the actuator is lightly affected by the presence of the main Mach 0.3 flow, we explored the effect of the actuation frequency on this flow. In an attempt to isolate the influence of frequency from that of amplitude, the actuator voltage was adjusted with the varying frequency so to maintain, as much as possible, a constant mean velocity of about 5 m/s at the forcing slot.

Figure 9 illustrates some relevant forced cases in comparison with the baseline case at different frequencies. In all figures the thin line, representing the original Mach 0.3 cavity-flow spectrum, is displaced 20 dB above the forced one to avoid the overlapping of important spectral features. The baseline flow is characterized by a single resonant peak of 132 dB at 2.8 kHz. With forcing at 2.0 kHz, Fig. 9 (a), the resonant peak is suppressed while a strong peak appears at the actuation frequency, an indication that the natural feedback has been interrupted and the system has been tuned at the actuator frequency. As expected, actuation at the resonant frequency, Fig. 9 (b), has the effect of reinforcing the natural feedback and increases the resonant peak by about 8 dB. However forcing at 3.0 kHz, a frequency just slightly above resonance, Fig. 9 (c), produces the same effect noticed in Fig. 9 (a), the system being tuned at the forcing frequency with disruption of the resonant feedback loop. The same effect has been observed with forcing at the majority of frequencies between 2000 and 5000 Hz. In fact the actuator exhibited good authority even at the frequencies of the “valleys” of Figs. 7 and 8 where the forcing velocity appears to be rather low. An interesting case is presented in Fig. 9 (d) where actuation at 3.25 kHz reduced the resonant peak by 18 dB without introducing a strong peak of its own. This occurrence, observed also in a milder form for actuation at 3.85 kHz (not presented here), is not yet understood and warrants specific future research. We hypothesize that forcing at some actuation frequencies switches the cavity flow from single-mode to multi-mode resonance (compare Fig. 9 (d) with Fig. 3 (c) or (d)) where energy is dispersed between more spectral peaks. As it is discussed by Rowley et al. (2003), it is

possible that the cavity instability characteristic has been switched from non-linear to linear via this forcing. Use of joint time-frequency analysis and visual imaging techniques should help to clarify the physics of this phenomenon. In any case, this interesting result has been used in designing the preliminary type of control for reducing the resonant peaks which is discussed in the next section. Conversely, forcing at frequencies above 5.0 kHz, e.g. 7.8 kHz in Fig. 9 (e), has little effect on the resonant peak that is reduced but remains comparable to the forcing one. Even higher frequencies show no effect on the resonant peak that remains practically unchanged alongside the forcing tone, as shown for actuation at 10.4 kHz in Fig. 9 (f). We finally observe that while the forcing frequency may significantly affect the resonant peak, it seems to have little or no effect on the other spectral components, particularly the low-frequency plateau.

6. A preliminary, logic-based active controller for reduction of cavity flow resonance

Based on what was discovered in Fig. 9 (d), we decided to develop an automated routine that finds the actuation frequencies, if any, for which at a given Mach number from 0.25 to 0.5 the spectral peaks were eliminated or reduced. This quite naturally evolved into the logic-based process illustrated in Fig. 10 that can be considered a preliminary type of controller for reducing cavity-flow resonance.

This controller explores the forcing frequency f_f within a specified range, for instance between 2000 and 5000 Hz with increments Δf of 50 Hz. At each value of f_f , the actuator is excited by the sinusoidal voltage signal of fixed amplitude:

$$V_f = A \sin(2\pi f_f t) \quad (2)$$

After a short time (50 ms) has passed to ensure the dying out of any transient phenomenon, the pressure fluctuations in the cavity are measured by the Kulite transducer in the cavity floor. The corresponding voltage signal is filtered, translated into normalized pressure values, and a SPL spectrum is then computed as explained in section 3. The controller then searches the maximum spectral value SPL_{\max} and compares it with a preset, desired value SPL_{set} . If $SPL_{\max} < SPL_{\text{set}}$, the controller has found a forcing frequency f_f for which the preset requirement is satisfied and therefore stops exploring other forcing frequencies and

maintains the excitation at the current value of f_f . Otherwise, the controller continues the exploration of forcing frequencies in the specified range. If no forcing frequency has been found for which the spectrum is below SPL_{set} , the controller settle for the forcing frequency $f_{f, \text{min-peak}}$ for which the lowest spectral peak has been observed and maintains excitation at that frequency.

In essence the controller operates in a closed-loop fashion until it has found a satisfying forcing frequency after which it converts to an open-loop scheme. In fact, the process above is embedded into an additional outer loop that continuously monitors the state of the overall system and triggers a new search if some significant changes are detected, like an increase of the spectral intensity or a variation of the flow Mach number. While this approach can hardly be classified as a closed-loop control scheme according to the established control theory, it nevertheless performed remarkably well in our experiments as it was able to find and maintain forcing frequencies reducing strong cavity-flow resonant peaks in the entire range of Mach number explored. Furthermore, it proved to be a powerful tool for extracting valuable information in a large range of forcing conditions as discussed next.

First of all, it should be noted that, as was already mentioned in the discussion of Fig. 9 (d), sometimes more than one forcing frequency f_f exists for which a significant peak reduction is achieved. From here on we restrict our discussion only to the forcing frequencies, which we call "optimal", for which the largest reduction has been observed.

In Fig. 11 the lines capture the "optimal" frequencies with actuator excitation voltages of 5, 4, 3, and 2 V_{rms} while the circles, similar to Fig. 2, represent the original resonant frequencies for cavity flow Mach number between 0.25 and 0.5. The optimal frequency somewhat varies with the excitation voltage at each Mach number, but a general trend is still recognizable, which is characterized by jumps at some Mach numbers. This is not completely surprising since, like other self-sustained resonant flows, the cavity resonance is distinguished by a staging behavior as evidenced by the nature of the Rossiter modes. Based on the results presented in this figure, a simpler controller, embedded into an outer loop continuously monitoring the system, could be devised that directly selects the optimal actuation frequency and voltage for each flow Mach number.

Figure 12 shows the effect of optimal frequency forcing on the same flow cases discussed in Fig. 3. For each Mach number case, the thin line shows the same spectrum as of Fig. 3, while the thick line indicates the spectrum with optimal forcing at $4 V_{rms}$. Similar to what noted in commenting about Fig. 9, forcing has major effect on the peaks but seems to have little or no effect on the spectral components other than the peaks.

Figure 13 compares the highest values of the spectral peak as a function of the Mach number for the unforced flow and for flow with optimal frequency forcing at excitation voltages of 5, 4, 3, and $2 V_{rms}$. The thin continuous and dotted lines show the unforced peak and the low-frequency noise plateau values as in Fig. 4. The thick lines refer to the forcing cases. This figure and Figs. 12 (a) to (d) clarify that optimal forcing eliminates altogether the resonant peaks in the Mach range 0.25-0.4 irrespective of the actuator excitation voltage, i.e. the velocity at the exit slot. The resulting flow is so devoid of any significant peak that the maximum spectral level basically coincides with the low-frequency noise plateau. At higher Mach number, especially above Mach 0.45, the original resonant peak is much stronger and only intense actuation at 4 or $5 V_{rms}$ is capable of producing a peak reduction of 10 dB. It is also important to note that forcing produces little benefit at Mach numbers for which low-intensity peaks at multi-mode resonance exist (e.g. Mach 0.32) as the system is already in a state comparable to that induced by the actuation at optimal frequency.

7. Conclusions

A set of experiments for characterizing and controlling the resonance induced by flow over a shallow cavity in the Mach number range of 0.25-0.5 has been presented. Survey of the baseline flow indicates that the flow operates in single-mode resonance in the Mach ranges 0.25-0.31 and 0.39-0.5 and multi-mode resonance in the intermediate range of 0.32-0.38. Resonant peaks are particularly intense at the higher Mach number settings.

A preliminary study of the actuator, limited to the characteristics at its output located just below the leading edge of the cavity, has been performed. The results indicate a non-linear behavior that is not

significantly influenced by the presence of an external, Mach 0.3 main flow.

Forcing the flow at different frequencies reveals that, despite its non-linear performance, the actuator has a strong authority in the frequency range of 2-5 kHz as it is able to disrupt the natural resonant loop and to either tune the flow acoustics to its own frequency or eliminate/substantially reduce all the peaks/modes. At higher frequencies the actuator progressively loses its authority.

At some frequencies the effect of actuation was to reduce the resonant peak without introducing a peak of its own. The physics of this phenomenon are not yet understood and warrant further future investigation. Based on these observations, a preliminary, logic-based type of controller has been devised that searches the optimal actuation frequency for resonant peak suppression according to a feedback scheme and then maintains the system in such a state. The controller proved to be effective in reducing strong resonant peaks in all the Mach number range explored.

Extensive data collected in conjunction with the control experiments identify for each Mach number the optimal forcing frequency for reducing the resonant peak. This produces spectra devoid of any significant peak for Mach numbers less than 0.4 irrespective of the actuation intensity. At higher Mach number significant reductions are obtained only through larger actuation excitation voltages (strong actuation).

Future work suggested by this study includes an accurate survey of the actuator behavior comprising velocity measurements at various locations downstream of the forcing slot. The physics leading to the resonant peak suppression discovered at some forcing frequencies warrant special attention and a specific study where joint time-frequency analysis as well as flow visualization techniques are used to clarify the phenomenon. Faster control schemes for reducing the resonant tones can be derived from the preliminary logic-based approach presented here. Among them a feed-forward scheme exploiting the optimal frequency forcing and a streamlined logic-based scheme where feedback information is derived directly from the timetraces of the pressure fluctuations.

Acknowledgements

The support of this work by the AFRL/VA and AFOSR through Collaborative Center of Control Science (Contract F33615-01-2-3154) is very much appreciated. We would like to thank the rest of the flow control team at CCCS, Prof. Hitay Ozbay, Drs. James Myatt, James DeBonis, Chris Camphouse, Onder Efe, and Edgar Caraballo and Xin Yuan. We thank Drs. Tom McLaughlin, Stefan Siegel, Kelly Cohen, David Williams, and Clancy Rowley for fruitful discussions. Finally we gratefully acknowledge the help of James Hileman and Subin Seturam in implementing the routines for data acquisition and flow control.

REFERENCES

1. Cabell, R. H., Kegerise, M. A., Cox, D. E., and Gibbs, G. P., "Experimental Feedback Control of Flow Induced Cavity Tones," AIAA Paper 2002-2497, June 2002.
2. Cain, A. B., Rubio, A. D., Bortz, D. M., Banks, H. T., and Smith, R. C., "Optimizing Control of Open Bay Acoustics," AIAA Paper 2000-1928, June 2000.
3. Cattafesta III, L.N., Garg, S., Choudhari, M., and Li, F., "Active Control of Flow-Induced Cavity Resonance", AIAA paper 97-1804, 1997.
4. Cattafesta III, L.N., Garg, S., Kegerise, M.S., and Jones, G.S., "Experiments on Compressible Flow-Induced Cavity Oscillations", AIAA paper 98-2912, June 1998.
5. Chen, F.-J., Yao, C., Beeler, G.B., Bryant, R.G., and Fox, R.L., "Development of Synthetic Jet Actuators for Active Flow Control at NASA Langley", AIAA paper 2000-2405, June 2000.
6. Gad-el-Hak, M., *Flow Control – Passive, Active, and Reactive Flow Management*, Cambridge University Press, New York, NY, 2000.
7. Guy, Y., McLaughlin, T. E., Albertson, J. A., "Effect of Geometric Parameter on the Velocity Output of a Synthetic Jet Actuator", AIAA Paper 2002-0126, January 2002.
8. Kastner, J. and Samimy, M., "Development and Characterization of Hartmann Tube Fluidic Actuators for High-Speed Flow Control," *AIAA Journal*, Vol. 40, No. 10, 2002, pp. 1926-1934.
9. Kegerise, M. A., Cattafesta, L. N., III, and Ha, C., "Adaptive Identification and Control of Flow-Induced Cavity Oscillations," AIAA Paper 2002-3158, June 2002.
10. McCormick, D.C., "Boundary Layer Separation Control with Directed Synthetic Jets", AIAA paper 2000-0519, January 2000.
11. Raman, G. and Kibens, V., "Active Flow Control Using Integrated Powered Resonance Tube Actuators," AIAA Paper 2001-3024, June 2001a.
12. Raman, G., Mills, A., Othman, S., and Kibens, V., "Development of Powered Resonance Tube Actuators for Active Flow Control," ASME FEDSM 2001-18273, 2001b.
13. Rockwell, D., and Naudascher, E., "Review – Self-Sustaining Oscillations of Flow Past Cavities", *Journal of Fluids Engineering – Transactions of the ASME*, vol. 100, 1978, pp. 152-165.
14. Rossiter, J.E., "Wind Tunnel Experiments on the Flow Over Rectangular Cavities at Subsonic and Transonic Speeds", RAE Tech. Rep. 64037, 1964 and Aeronautical Research Council Reports and Memoranda No. 3438, Oct. 1964.
15. Rowley, C. W., Williams, D. R., Colonius, T., Murray, R. M., MacMartin, D. G., and Fabris, D., "Model-Based Control of Cavity Oscillations Part II: System Identification and Analysis," AIAA Paper 2002-0972, January 2002.
16. Samimy, M., Debiassi, M., Caraballo, E., Özbay, H., Efe, M. Ö., Yuan, X., DeBonis, J., and Myatt, J. H., "Closed-Loop Active Flow Control – A Collaborative Approach," AIAA Paper 2003-0058, January 2003.
17. Schaeffler, N. W., Hepner, T. E., Jones, G. S., and Kegerise, M. A., "Overview of Active Flow Control Actuator Development at NASA Langley Research Center," AIAA Paper 2002-3159, June 2002.

18. Smith, B.L., and Glezer, A., "The formation and evolution of synthetic jets", *Physics of Fluids*, Vol. 10, No. 9, 1998, pp. 2281-2297.
19. Stanek, M., Sinha, N., Seiner, J., Pearce, B., and Jones, M., "High Frequency Flow Control – Suppression of Aero-Optics in Tactical Directed Energy Beam Propagation and the Birth of a New Model (Part I), AIAA Paper 2002-2272, May 2002.
20. Stanek, M. J., Raman, G., Ross, J. A., Odedra, J., Peto, J., Alvi, F., and Kibens, V., "High Frequency Acoustic Suppression – The Role of Mass Flow, The Notion of Superposition, And The Role of Inviscid Instability – A New Model (Part II)," AIAA Paper 2002-2404, June 2002.
21. Williams, D. R., Fabris, D., Iwanski, K., and Morrow, J., "Closed-Loop Control in Cavities with Unsteady Bleed Forcing," AIAA Paper 2000-0470, January 2000a.
22. Williams, D.R., Fabris, D., and Morrow, J., "Experiments on Controlling Multiple Acoustic Modes in Cavities", AIAA paper 2000-1903, June 2000b.

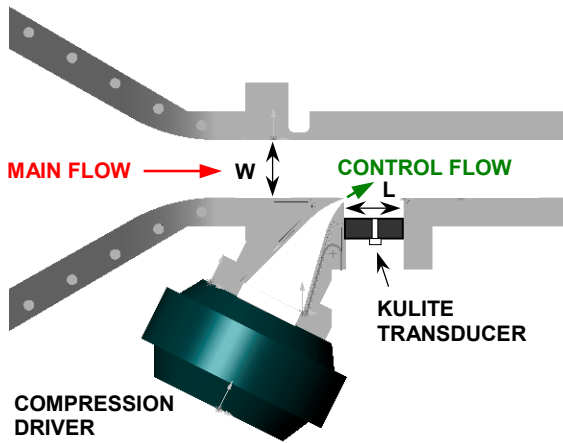


Figure 1: Cutout of the facility showing the converging nozzle, the test section, the cavity, the actuator layout, and the placement of the Kulite transducer.

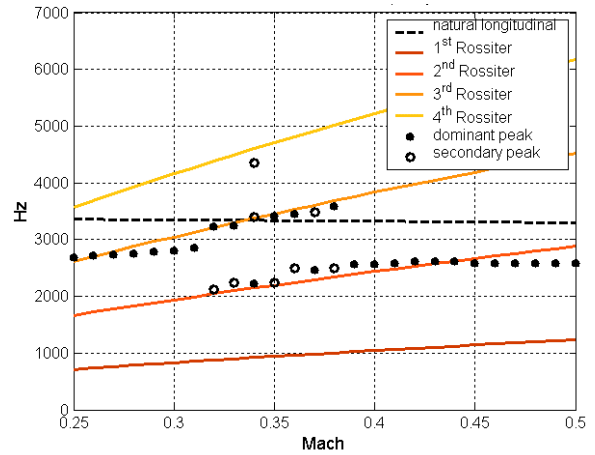


Figure 2: Rossiter frequencies (lines) and measured frequencies (circles) as a function of the flow Mach number.

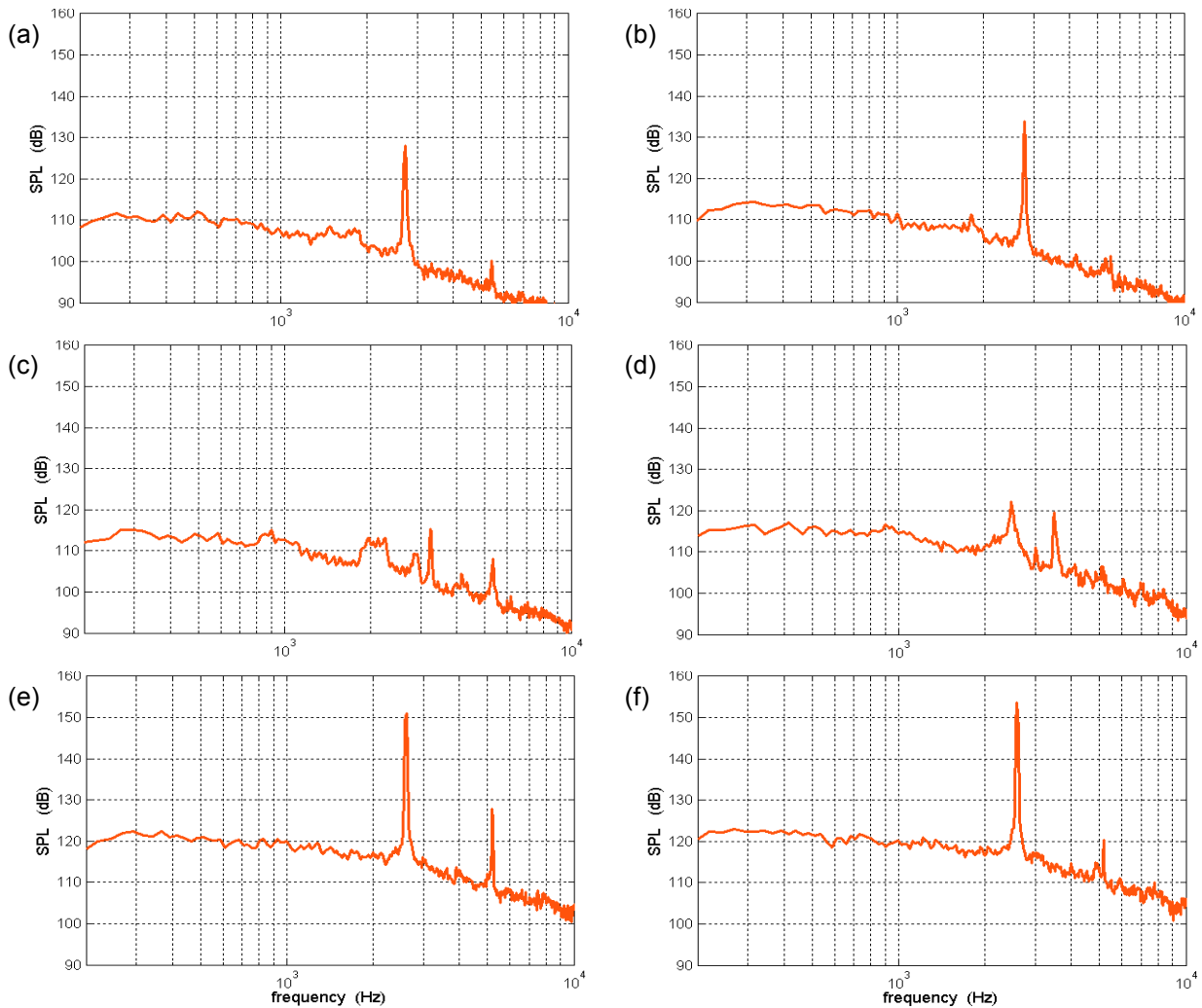


Figure 3: Cavity-flow pressure spectra at selected Mach numbers: (a) M = 0.26; (b) M = 0.29; (c) M = 0.32; (d) M = 0.37; (e) M = 0.43; (f) M = 0.46.

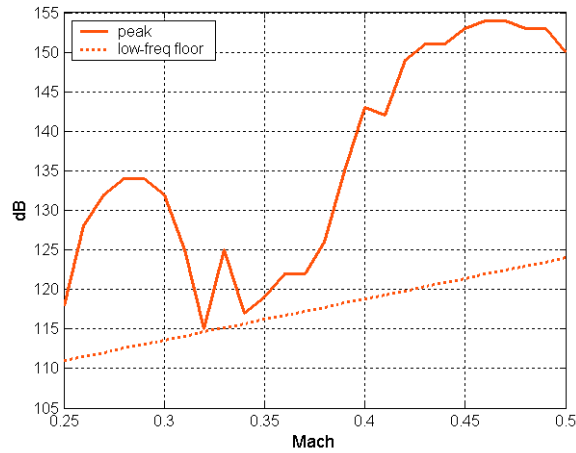


Figure 4: Intensity of the cavity-flow dominant pressure peak and of the low-frequency noise plateau as a function of the Mach number.

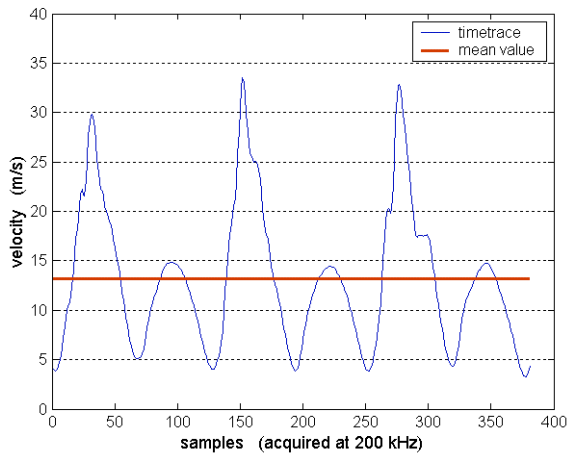


Figure 5: Timetrace and mean value of the velocity at the actuator exit slot for actuation at 1.6 kHz and excitation level of 5 V_{rms} in absence of main flow.

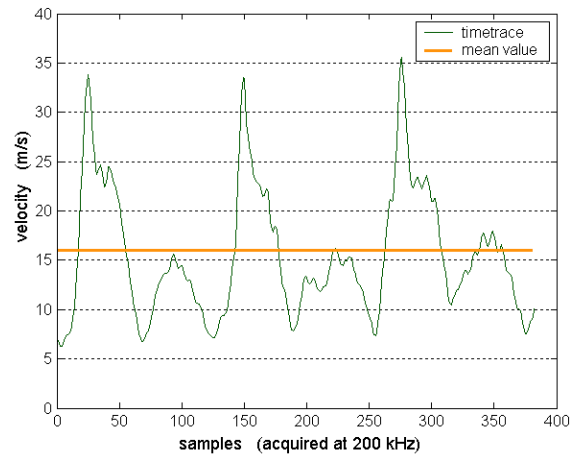


Figure 6: Timetrace and mean value of the velocity at the actuator exit slot for actuation at 1.6 kHz and excitation level of 5 V_{rms} in presence of Mach 0.3 main flow.

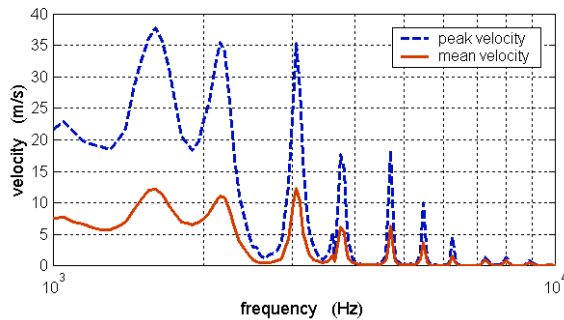


Figure 7: Variation of the peak and mean velocity at the actuator exit slot as a function of the actuation frequency for excitation level at 5 V_{rms} in absence of main flow.

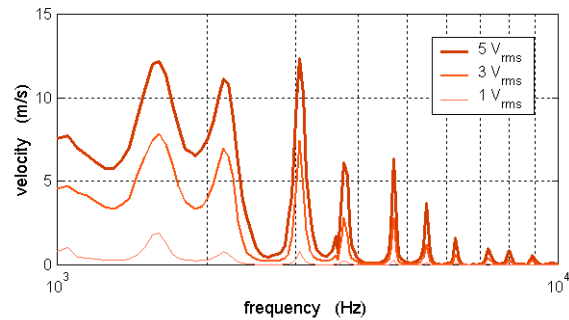


Figure 8: Variation of the mean velocity at the actuator exit slot as a function of the actuation frequency for excitation levels at 5, 3, and 1 V_{rms} in absence of main flow.

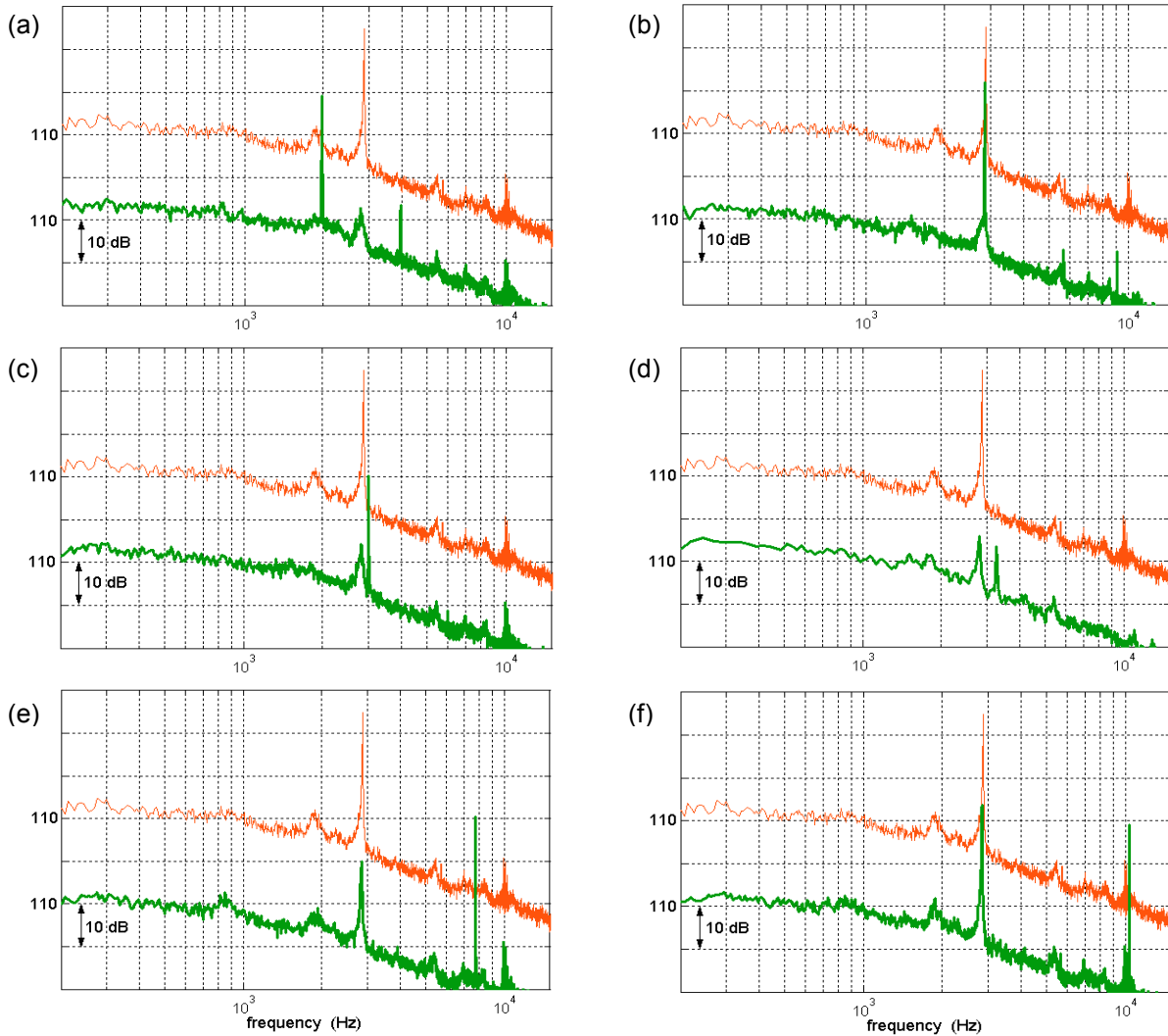


Figure 9: Effect of forcing frequency on Mach 0.3 flow; upper (thin) line is the baseline flow SPL spectrum and lower (thick) line is the spectrum with forcing at: (a) 2.0 kHz; (b) 2.8 kHz (resonant frequency); (c) 3.0 kHz; (d) 3.25 kHz; (e) 7.8 kHz; (f) 10.4 kHz.

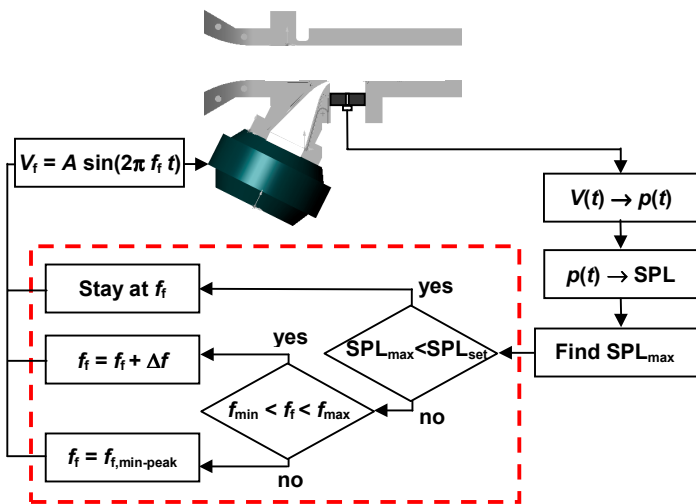


Figure 10: Schematics of the logic-based type of controller for reduction of cavity-flow resonant peaks.

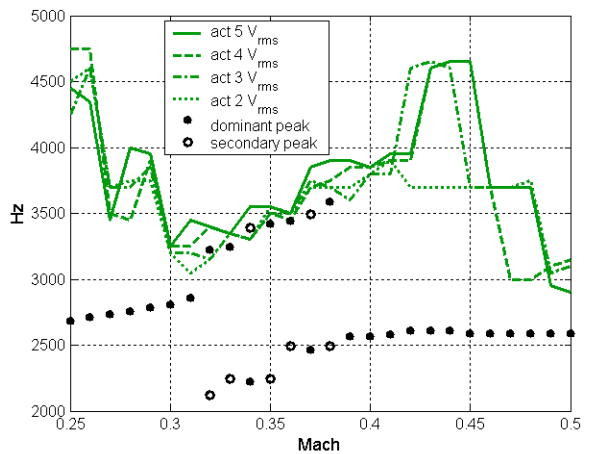


Figure 11: Peak frequencies and optimal forcing frequencies to reduce them as a function of the flow Mach number.

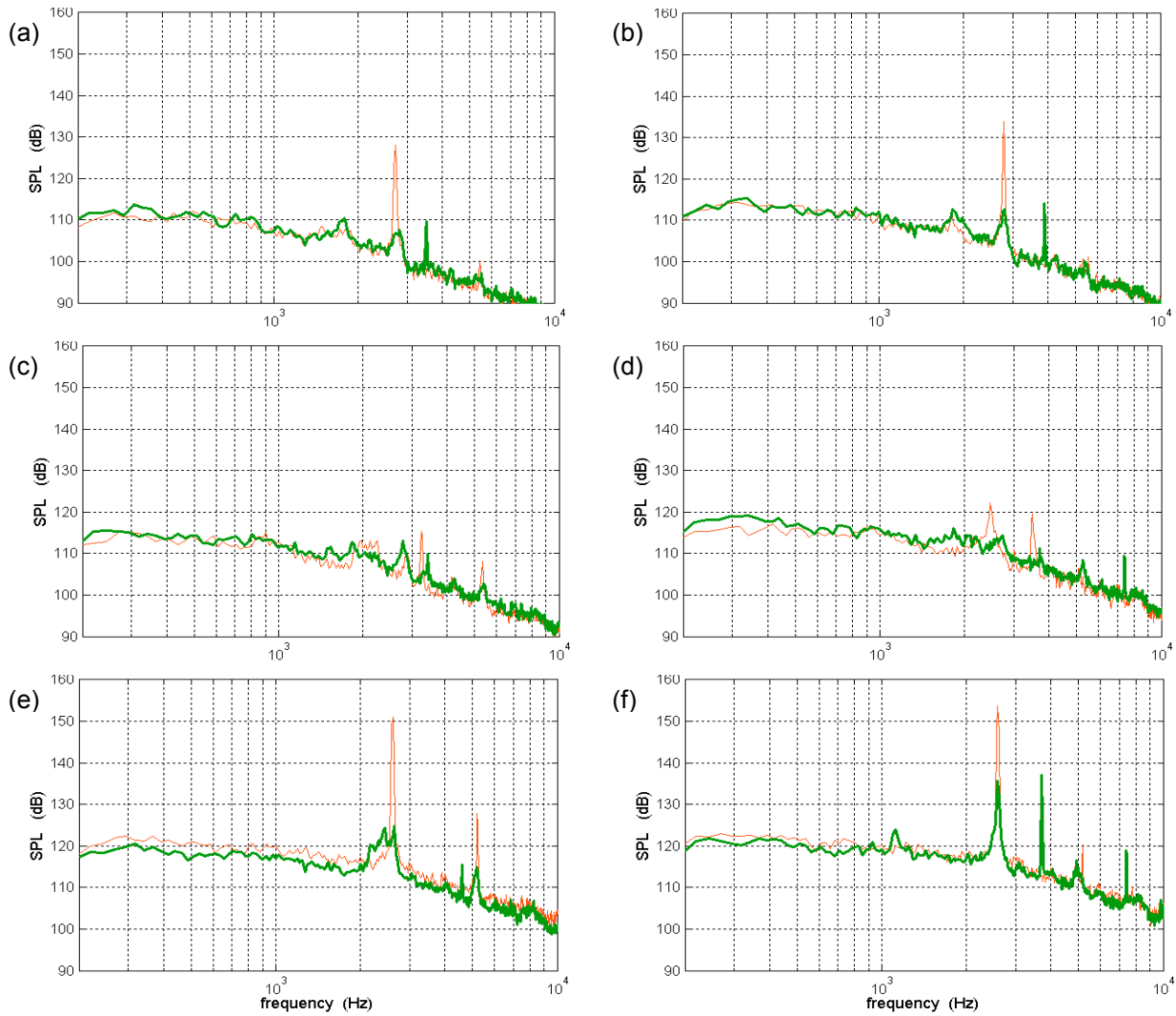


Figure 12: Noise spectra of the unforced cavity flow (thin line) and of the same flow controlled with optimal frequency forcing at $4 V_{rms}$ (thick line) at selected Mach numbers: (a) $M = 0.26$; (b) $M = 0.29$; (c) $M = 0.32$; (d) $M = 0.37$; (e) $M = 0.43$; (f) $M = 0.46$.

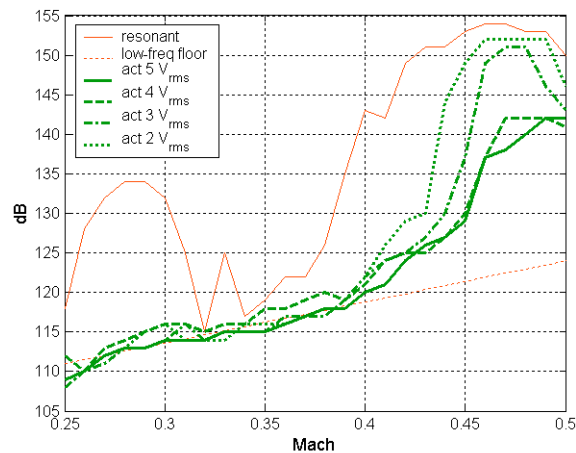


Figure 13: Intensity of the dominant peak for unforced flow and of the flow forced at optimal frequency for peak reduction as a function of the flow Mach number.